APOEε4 potentiates amyloid β effects on longitudinal tau pathology

João Pedro Ferrari-Souza[1,2], Bruna Bellaver[1], Pâmela C. Lukasewicz Ferreira[1], Andréa L. Benedet[3,4], Guilherme Povala[2], Firoza Z. Lussier[1,3], Douglas T. Leffa[1,5], Joseph Therriault[3], Cécile Tissot[1,3], Carolina Soares[1,2], Yi-Ting Wang[3], Mira Chamoun[3], Stijn Servaes[3], Arthur Cassa Macedo[3], Marie Vermeiren[3], Gleb Bezgin[3], Min Su Kang[3], Jenna Stevenson[3], Nesrine Rahmouni[3], Vanessa Pallen[3], Nina Margherita Poltronetti[3], Ann Cohen[1], Oscar L. Lopez[6], Dana L. Tudorascu[1], William E. Klunk[1], Victor L. Villemagne[1], Jean-Paul Soucy[7], Serge Gauthier[3], Diogo O. Souza[2], Thomas K. Karikari[1,4,8], Nicholas J. Ashton[4,9,10], Henrik Zetterberg[4,8,11,12,13], Kaj Blennow[4,8], Eduardo R. Zimmer[2,14,15], Pedro Rosa-Neto[3], and Tharick A. Pascoal[1,6]*

[1]Department of Psychiatry, School of Medicine, University of Pittsburgh, Pittsburgh, PA, USA.

[2]Graduate Program in Biological Sciences: Biochemistry, Universidade Federal do Rio Grande do Sul, Porto Alegre, RS, Brazil.

[3]Translational Neuroimaging Laboratory, McGill University Research Centre for Studies in Aging, Alzheimer's Disease Research Unit, Douglas Research Institute, Le Centre intégré universitaire de santé et de services sociaux (CIUSSS) de l'Ouest-de-l'Île-de-Montréal; Department of Neurology and Neurosurgery, Psychiatry and Pharmacology and Therapeutics, McGill University, Montreal, QC, Canada.

[4]Department of Psychiatry and Neurochemistry, The Sahlgrenska Academy at the University of Gothenburg, Mölndal, Sweden.

[5]ADHD Outpatient Program & Development Psychiatry Program, Hospital de Clínicas de Porto Alegre, Porto Alegre, RS, Brazil.

[6]Department of Neurology, School of Medicine, University of Pittsburgh, Pittsburgh, PA, USA

[7]Montreal Neurological Institute, McGill University, Montreal, QC, Canada.

[8]Clinical Neurochemistry Laboratory, Sahlgrenska University Hospital, Gothenburg, Sweden.

[9]Centre for Age-Related Medicine, Stavanger University Hospital, Stavanger, Norway.

[10]Department of Old Age Psychiatry, Institute of Psychiatry, Psychology & Neuroscience, King's College London, London, UK.

[11]Department of Neurodegenerative Disease, UCL Queen Square Institute of Neurology, London, UK.

[12]UK Dementia Research Institute at UCL, London, UK.

[13]Hong Kong Center for Neurodegenerative Diseases, Hong Kong, China.

[14]Department of Pharmacology, Universidade Federal do Rio Grande do Sul, Porto Alegre, RS, Brazil.

[15]Graduate Program in Biological Sciences: Pharmacology and Therapeuctis, Universidade Federal do Rio Grande do Sul, Porto Alegre, RS, Brazil.

*Correspondence to Tharick A. Pascoal, MD. PhD.

Departments of Psychiatry and Neurology, School of Medicine, University of Pittsburgh, Pittsburgh, PA, USA

3501 Forbes Avenue – Oxford Building, 15213, Pittsburgh, PA, USA

E-mail: PASCOAL@pitt.edu / Tel: (+1) 412-246-5147

Abstract

The mechanisms by which the apolipoprotein E ε4 (APOEε4) allele influences the pathophysiological progression of Alzheimer's disease (AD) are poorly understood. Here we tested the association of APOEε4 carriership and amyloid-β (Aβ) burden with longitudinal tau pathology. We longitudinally assessed 94 individuals across the aging and AD spectrum who underwent clinical assessments, APOE genotyping, magnetic resonance imaging, positron emission tomography (PET) for Aβ ([18F]AZD4694) and tau ([18F]MK-6240) at baseline, as well as a 2-year follow-up tau-PET scan. We found that APOEε4 carriership potentiates Aβ effects on longitudinal tau accumulation over 2 years. The APOEε4-potentiated Aβ effects on tau-PET burden were mediated by longitudinal plasma phosphorylated tau at threonine 217 (p-tau217+) increase. This longitudinal tau accumulation as measured by PET was accompanied by brain atrophy and clinical decline. Our results suggest that the APOEε4 allele plays a key role in Aβ downstream effects on the aggregation of phosphorylated tau in the living human brain.

Keywords: Alzheimer's disease; apolipoprotein E ε4; amyloid-β; tau; biomarkers; neuroimaging.

Introduction

Alzheimer's disease (AD) is characterized by the progressive accumulation of amyloid-β (Aβ) plaques and tau neurofibrillary tangles (1, 2), which are the main suspects of promoting neuronal loss and cognitive impairment (3). Although the *ε4* variant of the apolipoprotein E (*APOE*) gene is the main genetic risk factor for sporadic AD (4-7), how the *APOE*ε4 genotype impacts the pathogenesis of this neurodegenerative condition is still not fully understood (8). Interestingly, rather than just driving the increase of Aβ burden (9), recent observations have implicated the *APOE*ε4 genotype in potentiating the downstream effects of Aβ burden on cognitive deterioration (10-12). In addition, evidence from animal studies indicates that the *APOE*ε4 allele might influence the association of Aβ with cognition by contributing to tau pathogenesis (13-15). Accordingly, cross-sectional human investigations have suggested an interaction of *APOE*ε4 and Aβ on tau pathology (16, 17). Tracking the longitudinal association of *APOE*ε4 and Aβ pathology with tau pathology progression in living individuals is a critical next step to better understand the multifaced role of the *APOE*ε4 allele in the development of AD pathophysiology and may provide insights into the biological definition of the disease (18).

Here, using imaging and fluid biomarkers for the quantification of Aβ burden and tau pathology progression, we tested the hypothesis that *APOE*ε4 carriership is key to determining the deleterious effects of Aβ on the accumulation of hyperphosphorylated tau in the form of neurofibrillary tangles. In addition, we also investigated whether the aforementioned effects parallel neurodegeneration and clinical decline.

Materials and methods

Participants

Data were derived from the Translational Biomarkers in Aging and Dementia (TRIAD) cohort (https://triad.tnl-mcgill.com), an ongoing longitudinal and prospective study of aging and AD. Study participants were recruited from the community or the McGill University Research Centre for Studies in Aging through advertisements, printed materials, word of mouth, and referrals. Individuals were not eligible for inclusion if presenting inadequate visual and auditory capacities for neuropsychologic assessment, inability to speak English or French, magnetic resonance imaging (MRI) or positron emission tomography (PET) safety contraindications, recent head trauma, major surgery, active substance abuse, or inadequately treated neurological, psychiatric, or systemic conditions. All study participants provided written informed consent. The study was approved by the Montreal Neurological Institute PET Working Committee and the Douglas Mental Health University Institute Research Ethics Board.

Our cohort consisted of TRIAD participants across the aging and AD clinical spectrum who underwent clinical assessments, *APOE* genotyping, MRI, Aβ-PET, and tau-PET at baseline, as well as a follow-up tau-PET at least 1.5 years after baseline. CU individuals had a global Clinical Dementia Rating Scale (CDR) score of 0 and no objective cognitive impairment. Participants with MCI had a global CDR score of 0.5, subjective and objective cognitive impairments, and preserved activities of daily living (19). Patients with sporadic late-onset AD dementia had a global CDR score from 0.5 to 2 and fulfilled the National Institute on Aging and the Alzheimer's Association (NIA-AA) criteria for probable AD (20). In contrast with *APOE*ε4, the *APOE*ε2 allele has been reported to protect against AD development (21). Thus, similar to previous studies (22), we did not include individuals bearing the *APOE*ε2 allele in our aged population to increase the reliability of our *APOE*ε4-related results.

Blood biomarker and *APOE* genotype

Plasma phosphorylated tau at threonine 217 enhanced by additional phosphorylated sites (p-tau217^{+}) levels was quantified on the Single Molecular Array (Simoa) HD-X platform by Janssen R&D (23). Plasma p-tau217^{+} values below the lower limit of detection (0.013 pg/mL) were excluded. Values within the lower limit of detection (0.013 pg/mL) and lower limit of quantification (0.04 pg/mL) were only included if measured in duplicate with a coefficient of variation (CV) < 20%. *APOE* genotype was performed using the polymerase chain reaction amplification technique, followed by restriction enzyme digestion, standard gel resolution, and visualization processes. A more detailed description of the genotyping procedure is described elsewhere (24).

Image acquisition and processing

T1-weighted magnetization prepared rapid acquisition gradient echo MRI data were acquired on a 3T Siemens Magnetom at the Montreal Neurological Institute (repetition time: 2300 ms; echo time: 2.96ms; flip angle: 9°, coronal orientation perpendicular to the double spin echo sequence; 1x1 mm^2 in-plane resolution of 1 mm slab thickness) (25). Brain atrophy was assessed with gray matter (GM) density on T1-weighted MRI using voxel-based morphometry. PET data were acquired on a brain-dedicated Siemens High-Resolution Research Tomograph at the Montreal Neurological Institute. Aβ-PET images were acquired 40–70 min after the intravenous bolus injection of the [^{18}F]AZD4694 radiotracer, and scans were reconstructed with the ordered subset expectation maximization (OSEM) algorithm on a four-dimensional (4D) volume with three frames (3 x 600 seconds) (26). Tau-PET images were acquired 90–110 min after the intravenous bolus injection of the [^{18}F]MK-6240 radiotracer, and scans were reconstructed using the same OSEM algorithm on a 4D volume with four frames (4 x 300 seconds) (26).

Following each PET acquisition, a 6-min transmission scan with a rotating ^{137}Cs point source was performed for attenuation correction. PET images underwent additional correction for motion, dead time, decay, and random and scattered coincidences. Non-uniformity and field distortion corrections were performed for T1-weighted MRI images. Next, PET images were automatically registered to the native T1-weighted MRI, and the T1-weighted MRI images were linearly and nonlinearly registered to the Alzheimer's Disease Neuroimaging Initiative (ADNI) template space. Using the transformation parameters from the PET registration to the correspondent T1-weighted MRI and the T1-weighted MRI registration with the ADNI space, PET images were then linearly and nonlinearly registered to the ADNI space. All images were visually inspected to ensure proper alignment with the ADNI template. Of note, tau-PET images were meninges-stripped in native space before transformations or blurring to minimize the influence of meningeal spillover in adjacent brain regions (27). The PET images were spatially smoothed to achieve a final resolution of 8 mm full width at half-maximum. Aβ-PET SUVR maps were generated using the whole cerebellum gray matter as the reference region (28). In accordance with previous longitudinal tau-PET studies (29, 30), tau-PET SUVR maps were generated using the cerebellar crus I gray matter (derived from the SUIT cerebellum atlas) (31) as the reference region. A global neocortical Aβ-PET SUVR was estimated from the precuneus, prefrontal, orbitofrontal, parietal, temporal, and cingulate cortices (32). According to a previously published threshold, Aβ positivity (Aβ+) was determined as global Aβ-PET SUVR > 1.55 (33). A summary measure of tau-PET SUVR was estimated in a temporal meta-ROI comprising the entorhinal, hippocampal, fusiform, parahippocampal, inferior temporal, and middle temporal cortices (32). CU young adults (20 to 25 years) were used to determine tau tangle longitudinal accumulation status. Participants were classified as tau tangle accumulators

if the tau-PET SUVR rate of change in the temporal meta-ROI was 2 SDs above the mean from the CU young population (34).

Statistical analysis

Demographic differences were assessed using analysis of variance (continuous variables) and contingency $\chi 2$ test (categorical variables). Annualized measures of change for AD markers were calculated as the difference between follow-up and baseline divided by time. Outliers were identified using Rosner's test (R package "EnvStats" (35)). Analysis of covariance (ANCOVA) with Tukey's multiple comparisons test assessed group differences. The relationship of tau tangle accumulation status with *APOE*ε4 and Aβ-PET was assessed using logistic regression. Voxel-wise and ROI-based linear regressions tested the interaction and main effects of *APOE*ε4 and Aβ-PET on longitudinal tau-PET and plasma p-tau217$^+$. Linear regressions also assessed the associations of longitudinal tau-PET accumulation with changes in plasma p-tau217$^+$ levels, GM density, and CDR-SB score. Sensitivity analyses were conducted to evaluate the potential confounding effect of baseline levels of the AD markers being assessed. Continuous predictors were standardized, and models were adjusted for age, sex, diagnosis, and years of education (if assessing GM density or CDR-SB score). Multiple comparisons correction at $P < 0.05$ was conducted using random field theory (RFT) (36) for voxel-wise analysis. Models were compared using the R-squared and Akaike Information Criterion (AIC). Mediation models investigated the association between Aβ-PET, plasma p-tau217$^+$, and tau-PET. Statistics were performed in R version 4.0.2 (http://www.r-project.org/). Imaging analyses were carried out using the R package "RMINC" (37). A 2-tailed *P*-value < 0.05 was considered statistically significant.

Results

We studied 107 individuals (10 CU young, 62 CU elderly, 25 MCI, and 10 sporadic late-onset AD dementia) with longitudinal tau-PET (mean [SD] follow-up, 2.3 [0.5] years). Demographic characteristics of our aged population (55 to 85 years) are shown in **Table 1** and of our CU young population (20 to 25 years) in **Supplementary Table 2**. There was no statistically significant difference between CU elderly, MCI, and AD dementia individuals regarding age, sex, years of education, *APOE*ε4 status, and time of follow-up.

Co-occurrence of *APOE*ε4 and Aβ+ associates with faster tau tangle accumulation

The annual rate of change in tau-PET SUVR was assessed across groups defined at baseline based on *APOE*ε4 and Aβ statuses. Six outliers were identified and removed from subsequent analysis. Average voxel-wise maps revealed that Aβ+ *APOE*ε4 carriers presented faster and more widespread tau-PET accumulation rates in relation to the other groups (**Figure 1**). ANCOVA model adjusted for age, sex, and diagnosis confirmed that the Aβ+ *APOE*ε4 carrier group had significantly faster rates of temporal meta-ROI tau-PET SUVR increase compared to all other groups (*vs.* Aβ- *APOE*ε4 noncarrier: $P = 0.002$; *vs.* Aβ- *APOE*ε4 carrier: $P = 0.003$; *vs.* Aβ+ *APOE*ε4 noncarrier: $P = 0.020$; **Figure 2A**). By contrast, no significant differences were observed among the Aβ- *APOE*ε4 noncarrier, Aβ- *APOE*ε4 carrier, and Aβ+ *APOE*ε4 noncarrier groups ($P \geq 0.621$; **Figure 2A**). Logistic regression further supported that only the concomitant presence of Aβ+ and *APOE*ε4 carriership was associated with tau tangle accumulation ($P = 0.016$; **Figure 2B** and **C**).

*APOE*ε4 determines Aβ effects on tau tangle accumulation

We next tested the interaction and main effects of *APOE*ε4 status and global Aβ-PET burden on longitudinal tau-PET accumulation adjusting for age, sex, and diagnosis. ROI-based linear regression analysis revealed a significant interaction effect between *APOE*ε4 and global Aβ-PET load on longitudinal tau-PET SUVR increase in the temporal meta-ROI (β = 0.027, 95% confidence interval [CI] 0.009 to 0.044, $P = 0.003$; **Figure 2D** and **Supplementary Table 3**) in the absence of significant main effects ($P \geq 0.347$; **Figure 2D** and **Supplementary Table 3**). Sensitive analysis supported that these effects were independent of baseline tau-PET uptake (**Supplementary Table 4**). Model comparisons showed that longitudinal tau-PET accumulation was better explained by the model including the interaction between global *APOE*ε4 and Aβ-PET in comparison to models including *APOE*ε4 only, Aβ-PET only, and both *APOE*ε4 and Aβ-PET (**Figure 2E**).

We next investigated the topography of the interaction effects of *APOE*ε4 and Aβ on longitudinal tau-PET uptake across the brain. Voxel-wise linear regression analysis demonstrated that the interaction between global Aβ-PET burden and *APOE*ε4 carriership was significantly associated with faster rates of increase in tau-PET uptake in classical brain regions of tau tangle deposition, such as temporoparietal areas (**Figure 2F**). Notably, *APOE*ε4 and Aβ joint effects were mainly observed in neocortical areas comprising Braak III-VI (**Supplementary Figure 1**).

*APOE*ε4 potentiates Aβ effects on tangles through tau hyperphosphorylation

We assessed whether tau hyperphosphorylation, measured with plasma ptau217^{+} changes, could explain *APOE*ε4 and Aβ interaction effects on 2-year tau-PET accumulation. In a regression model accounting for covariates, we found that the interaction between

*APOE*ε4 carriership and global Aβ-PET burden, rather than their main effects, was associated with longitudinal plasma ptau217^{+} increase (β = 0.017, 95% CI 0.004 to 0.030, *P* = 0.010; **Figure 3A**). Sensitive analysis indicated that these effects were independent of baseline plasma p-tau217^{+} levels (**Supplementary Table 5**). Furthermore, plasma p-tau217^{+} change was significantly related to tau-PET SUVR change in the brain regions showing *APOE*ε4 and Aβ joint effects on longitudinal tau-PET accumulation (β = 0.033, 95% CI 0.022 to 0.44, *P* < 0.001; **Figure 3B** and **Supplementary Table 6**). By contrast, no association was observed outside these brain regions (**Figure 3C** and **Supplementary Figure 2**). Mediation analyses confirmed that Aβ-PET effects on 2-year tau-PET accumulation occurred through the longitudinal increase of plasma p-tau217^{+} levels in *APOE*ε4 carriers (**Figure 3D)** but not in *APOE*ε4 noncarriers **Figure 3E**).

Tau tangle accumulation parallels neurodegeneration and clinical decline.

We tested whether tau-PET accumulation in the regions showing *APOE*ε4 and Aβ interaction effects on tau-PET accumulation was accompanied by local brain atrophy (indexed by GM density) and clinical deterioration (measured with the CDR-SB score) adjusting for age, sex, diagnosis, and years of education. We found that longitudinal tau-PET accumulation was associated with higher rates of local GM density decrease (β = -0.0009, 95% CI -0.0018 to -0.0001, *P* = 0.034; Model A in **Table 2**). Tau-PET deposition was also associated with higher rates of CDR-SB increase (β = 0.150, 95% CI 0.037 to 0.263, *P* = 0.010; Model B in **Table 2**). Sensitivity analyses accounting for the potential confounding effect of baseline GM density levels and CDR-SB score showed similar findings (**Supplementary Table 7**).

Discussion

The results from the present study support that the *APOE*ε4 genotype drives Aβ effects on the longitudinal brain accumulation of neurofibrillary tangles through tau hyperphosphorylation at threonine 217. This longitudinal tau tangle accumulation was paralleled by brain atrophy and clinical deterioration.

*APOE*ε4 carriership potentiated Aβ effects on tau tangle accumulation over two years across the AD spectrum. Our results are supported by previous neuropathological evidence showing that the association between *APOE*ε4 and tau tangles is stronger in the presence of Aβ pathology (17). A recent cross-sectional study also reported that *APOE*ε4 modulates the association of Aβ and tau in living AD patients (16). Here, we built on these observations by providing evidence that the *APOE*ε4 allele drives Aβ effects on the subsequent aggregation of tau phosphorylated into neurofibrillary tangles. It has been reported that Aβ deposition is more closely related to cognitive decline (10-12) in *APOE*ε4 carriers than in *APOE*ε4 noncarriers. Our results suggest that this observation may be explained by the fact that *APOE*ε4 exacerbates Aβ effects on tau tangles, which in turn promotes neurodegeneration and clinical deterioration. Here, we propose that, beyond its well-established contribution to Aβ aggregation (9), *APOE*ε4 also potentiates Aβ effects on tau pathology. These findings have important implications for the design of future clinical trials. It could suggest that intervention trials testing drug effects on tau tangles deposition may benefit from considering both *APOE*ε4 and Aβ statuses as enrollment criteria to select individuals at higher risk of fast tau tangle accumulation. Furthermore, the two hits of *APOE*ε4 also support that the development of combination therapies targeting ApoeE4 and Aβ pathology has the potential to synergistically halt tau progression in AD.

Our results indicate that the *APOE*ε4 is a key player in the fast accumulation of tau tangles in regions outside the temporal cortex. Specifically, we found that *APOE*ε4 drives Aβ-dependent deposition of tau in neocortical regions. Accumulation of tau tangles in the medial temporal cortex is often found in cognitively intact individuals (38, 39), whereas widespread accumulation over the neocortex is usually related to dementia symptoms (27, 40, 41). Although it has been widely proposed that Aβ pathology triggers the spread of tau over the neocortex (42), transcriptomic data demonstrated that *APOE* expression also has a pivotal role in tau spreading (43). Our findings corroborate both these notions, suggesting that the *APOE*ε4 allele catalyzes the Aβ-dependent spread of tau tangles outside the temporal lobe. Additionally, *APOE*ε4-potentiated Aβ effects on neocortical tau deposition were associated with brain atrophy and clinical decline, which further support that this phenomenon is key to the development of dementia (27, 41). Importantly, our results do not exclude *APOE*ε4-independent effects of Aβ on tau pathology but suggest that they are mild in a 2-year follow-up period.

We observed that *APOE*ε4-potentiated Aβ effects on tau tangles occurred through pathological tau phosphorylation at threonine 217. Initially, fluid p-tau and tau-PET have been proposed to be interchangeable biomarkers for detecting tau pathology (3). In contrast with this concept, recent studies demonstrated that fluid p-tau usually becomes abnormal in the absence of tau-PET positivity (44-47) and is more closely related to brain Aβ than tau tangle deposition. It is believed that during AD progression, tau protein becomes hyperphosphorylated in response to Aβ pathology and, subsequently, aggregates into neurofibrillary tangles (48). Therefore, a reasonable explanation for the temporal difference between fluid and imaging tau biomarkers is the fact that p-tau measures soluble and non-aggregated phosphorylated tau fragments, while tau-PET detects insoluble neurofibrillary tangles (49). Our results support this evolving framework in

which tau protein undergoes pathological phosphorylation in response to Aβ pathology and, subsequently, this hyperphosphorylated tau is the substrate to neurofibrillary tangle formation (49). In addition, we found that this phenomenon seems to explain, at least partially, the biological underpinnings of *APOE*ε4 and Aβ joint effects on neurofibrillary tangle accumulation. Taken together, these observations support a model where *APOE*ε4 is a key player in tau hyperphosphorylation and tangle formation.

Methodological limitations of the present study should be considered to interpret our results. A few of our analyses used thresholds to define biomarker positivity. Thresholds are always subject to conceptual and analytical idiosyncrasies as biomarkers naturally provide continuous values. Therefore, the use of different approaches to defining threshold values could change some of our findings. A potential source of self-selection bias is the fact that the study population was composed of volunteers motivated to participate in a study about dementia. Our study population had a limited number of *APOE*ε4 homozygotes, which precluded the analysis of a possible gene-dose effect. It would be highly desirable to study an *APOE*ε4 gene-dose effect in a populational-based cohort with a higher sample of *APOE*ε4 homozygotes. Future multicenter studies with longer follow-up intervals and multiple time points are needed to better characterize the temporal relationships between *APOE*ε4, Aβ, and tau across the AD spectrum.

To conclude, our results support that *APOE*ε4 genotype potentiates Aβ deleterious effects on hyperphosphorylation and accumulation of tau in the form of neurofibrillary tangles in AD.

Data availability

The data used in the present work is not publicly available as the information could compromise the participants' privacy. Therefore, the data from the TRIAD study will be made available from the senior authors upon reasonable request, and such arrangements are subject to standard data-sharing agreements.

Acknowledgments:

We acknowledge all study participants and the McGill Center for Studies in Aging staff. We also thank Dean Jolly, Alexey Kostikov, Monica Samoila-Lactatus, Karen Ross, Mehdi Boudjemeline, and Sandy Li for assisting in the radiochemistry production, as well as Richard Strauss, Edith Strauss, Guylaine Gagne, Carley Mayhew, Tasha Vinet-Celluci, Karen Wan, Sarah Sbeiti, Meong Jin Joung, Miloudza Olmand, Rim Nazar, Hung-Hsin Hsiao, Reda Bouhachi, and Arturo Aliaga for helping with the acquisition of the data.

Funding

This research is supported by the Alzheimer's Association (NIRG-12-92090 and NIRP-12-259245; PR-N), Brain Canada Foundation (CFI Project 34874; 33397; PR-N), Canadian Consortium of Neurodegeneration and Aging (MOP-11-51-31 - team 1; PR-N), Canadian Institutes of Health Research (MOP-11-51-31; RFN 152985, 159815, 162303; PR-N), Fonds de Recherche du Québec – Santé (Chercheur Boursier, 2020-VICO-279314; PR-N), and Weston Brain Institute (PR-N). TAP is supported by the National Institute of Health (R01AG075336 and R01AG073267) and the Alzheimer's Association (AACSF-20-648075). JPF-S receives financial support from CNPq (200691/2021-0). BB receives financial support from CAPES (88887.336490/2019-00) and Alzheimer's Association (AARFD-22-974627).

Competing interests:

SG has served as a scientific advisor to Cerveau Therapeutics. HZ has served at scientific advisory boards and/or as a consultant for Abbvie, Alector, Annexon, Apellis, Artery Therapeutics, AZTherapies, CogRx, Denali, Eisai, Nervgen, Novo Nordisk, Pinteon Therapeutics, Red Abbey Labs, reMYND, Passage Bio, Roche, Samumed, Siemens Healthineers, Triplet Therapeutics, and Wave, has given lectures in symposia sponsored by Cellectricon, Fujirebio, Alzecure, Biogen, and Roche, and is a co-founder of Brain Biomarker Solutions in Gothenburg AB (BBS), which is a part of the GU Ventures Incubator Program. KB has served as a consultant, at advisory boards, or at data monitoring committees for Abcam, Axon, BioArctic, Biogen, JOMDD/Shimadzu. Julius Clinical, Lilly, MagQu, Novartis, Prothena, Roche Diagnostics, and Siemens Healthineers, and is a co-founder of Brain Biomarker Solutions in Gothenburg AB (BBS), which is a part of the GU Ventures Incubator Program. ERZ serves on the scientific advisory board of Next Innovative Therapeutics. All other authors declare that they have no competing interests.

References

1. Polanco JC, Li C, Bodea LG, Martinez-Marmol R, Meunier FA, Gotz J. Amyloid-beta and tau complexity - towards improved biomarkers and targeted therapies. Nat Rev Neurol. 2018;14(1):22-39.

2. Knopman DS, Amieva H, Petersen RC, Chetelat G, Holtzman DM, Hyman BT, et al. Alzheimer disease. Nat Rev Dis Primers. 2021;7(1):33.

3. Jack CR, Jr., Bennett DA, Blennow K, Carrillo MC, Dunn B, Haeberlein SB, et al. NIA-AA Research Framework: Toward a biological definition of Alzheimer's disease. Alzheimers Dement. 2018;14(4):535-62.

4. Farrer LA, Cupples LA, Haines JL, Hyman B, Kukull WA, Mayeux R, et al. Effects of age, sex, and ethnicity on the association between apolipoprotein E genotype and Alzheimer disease. A meta-analysis. APOE and Alzheimer Disease Meta Analysis Consortium. JAMA. 1997;278(16):1349-56.

5. Genin E, Hannequin D, Wallon D, Sleegers K, Hiltunen M, Combarros O, et al. APOE and Alzheimer disease: a major gene with semi-dominant inheritance. Mol Psychiatry. 2011;16(9):903-7.

6. Lambert JC, Ibrahim-Verbaas CA, Harold D, Naj AC, Sims R, Bellenguez C, et al. Meta-analysis of 74,046 individuals identifies 11 new susceptibility loci for Alzheimer's disease. Nat Genet. 2013;45(12):1452-8.

7. Corder EH, Saunders AM, Strittmatter WJ, Schmechel DE, Gaskell PC, Small GW, et al. Gene dose of apolipoprotein E type 4 allele and the risk of Alzheimer's disease in late onset families. Science. 1993;261(5123):921-3.

8. Zhao N, Liu CC, Qiao W, Bu G. Apolipoprotein E, Receptors, and Modulation of Alzheimer's Disease. Biol Psychiatry. 2018;83(4):347-57.

9. Holtzman DM, Herz J, Bu G. Apolipoprotein E and apolipoprotein E receptors: normal biology and roles in Alzheimer disease. Cold Spring Harb Perspect Med. 2012;2(3):a006312.

10. Lim YY, Villemagne VL, Pietrzak RH, Ames D, Ellis KA, Harrington K, et al. APOE epsilon4 moderates amyloid-related memory decline in preclinical Alzheimer's disease. Neurobiol Aging. 2015;36(3):1239-44.

11. Kantarci K, Lowe V, Przybelski SA, Weigand SD, Senjem ML, Ivnik RJ, et al. APOE modifies the association between Abeta load and cognition in cognitively normal older adults. Neurology. 2012;78(4):232-40.

12. Mormino EC, Betensky RA, Hedden T, Schultz AP, Ward A, Huijbers W, et al. Amyloid and APOE epsilon4 interact to influence short-term decline in preclinical Alzheimer disease. Neurology. 2014;82(20):1760-7.

13. Shi Y, Yamada K, Liddelow SA, Smith ST, Zhao L, Luo W, et al. ApoE4 markedly exacerbates tau-mediated neurodegeneration in a mouse model of tauopathy. Nature. 2017;549(7673):523-7.

14. Litvinchuk A, Huynh TV, Shi Y, Jackson RJ, Finn MB, Manis M, et al. Apolipoprotein E4 Reduction with Antisense Oligonucleotides Decreases Neurodegeneration in a Tauopathy Model. Ann Neurol. 2021;89(5):952-66.

15. Wang C, Xiong M, Gratuze M, Bao X, Shi Y, Andhey PS, et al. Selective removal of astrocytic APOE4 strongly protects against tau-mediated neurodegeneration and decreases synaptic phagocytosis by microglia. Neuron. 2021;109(10):1657-74 e7.

16. Therriault J, Benedet AL, Pascoal TA, Mathotaarachchi S, Savard M, Chamoun M, et al. APOEepsilon4 potentiates the relationship between amyloid-beta and tau pathologies. Mol Psychiatry. 2020.

17. Farfel JM, Yu L, De Jager PL, Schneider JA, Bennett DA. Association of APOE with tau-tangle pathology with and without beta-amyloid. Neurobiol Aging. 2016;37:19-25.

18. Jack CR, Jr., Bennett DA, Blennow K, Carrillo MC, Dunn B, Haeberlein SB, et al. NIA-AA Research Framework: Toward a biological definition of Alzheimer's disease. Alzheimers Dement. 2018;14(4):535-62.

19. Petersen RC. Mild cognitive impairment as a diagnostic entity. J Intern Med. 2004;256(3):183-94.

20. McKhann GM, Knopman DS, Chertkow H, Hyman BT, Jack CR, Jr., Kawas CH, et al. The diagnosis of dementia due to Alzheimer's disease: recommendations from the National Institute on Aging-Alzheimer's Association workgroups on diagnostic guidelines for Alzheimer's disease. Alzheimers Dement. 2011;7(3):263-9.

21. Yamazaki Y, Zhao N, Caulfield TR, Liu CC, Bu G. Apolipoprotein E and Alzheimer disease: pathobiology and targeting strategies. Nat Rev Neurol. 2019;15(9):501-18.

22. Montagne A, Nation DA, Sagare AP, Barisano G, Sweeney MD, Chakhoyan A, et al. APOE4 leads to blood-brain barrier dysfunction predicting cognitive decline. Nature. 2020;581(7806):71-6.

23. Triana-Baltzer G, Moughadam S, Slemmon R, Van Kolen K, Theunis C, Mercken M, et al. Development and validation of a high-sensitivity assay for measuring p217+tau in plasma. Alzheimers Dement (Amst). 2021;13(1):e12204.

24. Saykin AJ, Shen L, Yao X, Kim S, Nho K, Risacher SL, et al. Genetic studies of quantitative MCI and AD phenotypes in ADNI: Progress, opportunities, and plans. Alzheimers Dement. 2015;11(7):792-814.

25. Ferrari-Souza JP, Ferreira PCL, Bellaver B, Tissot C, Wang Y-T, Leffa DT, et al. Astrocyte biomarker signatures of amyloid-β and tau pathologies in Alzheimer’s disease. Molecular Psychiatry. 2022.

26. Pascoal TA, Shin M, Kang MS, Chamoun M, Chartrand D, Mathotaarachchi S, et al. In vivo quantification of neurofibrillary tangles with [(18)F]MK-6240. Alzheimers Res Ther. 2018;10(1):74.

27. Pascoal TA, Therriault J, Benedet AL, Savard M, Lussier FZ, Chamoun M, et al. 18F-MK-6240 PET for early and late detection of neurofibrillary tangles. Brain. 2020;143(9):2818-30.

28. Cselenyi Z, Jonhagen ME, Forsberg A, Halldin C, Julin P, Schou M, et al. Clinical validation of 18F-AZD4694, an amyloid-beta-specific PET radioligand. J Nucl Med. 2012;53(3):415-24.

29. Jack CR, Jr., Wiste HJ, Schwarz CG, Lowe VJ, Senjem ML, Vemuri P, et al. Longitudinal tau PET in ageing and Alzheimer's disease. Brain. 2018;141(5):1517-28.

30. Pascoal TA, Benedet AL, Tudorascu DL, Therriault J, Mathotaarachchi S, Savard M, et al. Longitudinal 18F-MK-6240 tau tangles accumulation follows Braak stages. Brain. 2021.

31. Diedrichsen J, Balsters JH, Flavell J, Cussans E, Ramnani N. A probabilistic MR atlas of the human cerebellum. Neuroimage. 2009;46(1):39-46.

32. Jack CR, Jr., Wiste HJ, Weigand SD, Therneau TM, Lowe VJ, Knopman DS, et al. Defining imaging biomarker cut points for brain aging and Alzheimer's disease. Alzheimers Dement. 2017;13(3):205-16.

33. Therriault J, Benedet AL, Pascoal TA, Savard M, Ashton NJ, Chamoun M, et al. Determining Amyloid-beta Positivity Using (18)F-AZD4694 PET Imaging. J Nucl Med. 2021;62(2):247-52.

34. Therriault J, Pascoal TA, Benedet AL, Tissot C, Savard M, Chamoun M, et al. Frequency of Biologically Defined Alzheimer Disease in Relation to Age, Sex, APOE epsilon4, and Cognitive Impairment. Neurology. 2021;96(7):e975-e85.

35. Millard SP. EnvStats. 2 ed: Springer New York, NY; 2013. XVI, 291 p.

36. Worsley KJ, Taylor JE, Tomaiuolo F, Lerch J. Unified univariate and multivariate random field theory. Neuroimage. 2004;23 Suppl 1:S189-95.

37. Lerch J, Hammill C, van Eede M, Cassel D. RMINC: Statistical Tools for Medical Imaging NetCDF (MINC) Files 2017 [Available from: http://mouse-imaging-centre.github.io/RMINC.

38. Braak H, Braak E. Neuropathological stageing of Alzheimer-related changes. Acta Neuropathol. 1991;82(4):239-59.

39. Braak H, Braak E. Frequency of stages of Alzheimer-related lesions in different age categories. Neurobiol Aging. 1997;18(4):351-7.

40. Therriault J, Pascoal TA, Lussier FZ, Tissot C, Chamoun M, Bezgin G, et al. Biomarker modeling of Alzheimer's disease using PET-based Braak staging. Nature Aging. 2022;2(6):526-35.

41. Nelson PT, Alafuzoff I, Bigio EH, Bouras C, Braak H, Cairns NJ, et al. Correlation of Alzheimer disease neuropathologic changes with cognitive status: a review of the literature. J Neuropathol Exp Neurol. 2012;71(5):362-81.

42. Jack CR, Jr., Knopman DS, Jagust WJ, Petersen RC, Weiner MW, Aisen PS, et al. Tracking pathophysiological processes in Alzheimer's disease: an updated hypothetical model of dynamic biomarkers. Lancet Neurol. 2013;12(2):207-16.

43. Montal V, Diez I, Kim CM, Orwig W, Bueicheku E, Gutierrez-Zuniga R, et al. Network Tau spreading is vulnerable to the expression gradients of APOE and glutamatergic-related genes. Sci Transl Med. 2022;14(655):eabn7273.

44. Groot C, Smith R, Stomrud E, Binette AP, Leuzy A, Wuestefeld A, et al. Phospho-tau with subthreshold tau-PET predicts increased tau accumulation rates in amyloid-positive individuals. Brain. 2022.

45. Mattsson-Carlgren N, Andersson E, Janelidze S, Ossenkoppele R, Insel P, Strandberg O, et al. Abeta deposition is associated with increases in soluble and

phosphorylated tau that precede a positive Tau PET in Alzheimer's disease. Sci Adv. 2020;6(16):eaaz2387.

46. Barthelemy NR, Li Y, Joseph-Mathurin N, Gordon BA, Hassenstab J, Benzinger TLS, et al. A soluble phosphorylated tau signature links tau, amyloid and the evolution of stages of dominantly inherited Alzheimer's disease. Nat Med. 2020;26(3):398-407.

47. Reimand J, Collij L, Scheltens P, Bouwman F, Ossenkoppele R, Alzheimer's Disease Neuroimaging I. Association of amyloid-beta CSF/PET discordance and tau load 5 years later. Neurology. 2020;95(19):e2648-e57.

48. Querfurth HW, LaFerla FM. Alzheimer's disease. N Engl J Med. 2010;362(4):329-44.

49. Karikari TK, Ashton NJ, Brinkmalm G, Brum WS, Benedet AL, Montoliu-Gaya L, et al. Blood phospho-tau in Alzheimer disease: analysis, interpretation, and clinical utility. Nat Rev Neurol. 2022;18(7):400-18.

Table 1. Study participant characteristics.

	CU elderly	MCI	AD	*P*-value
No.	62	25	10	-
Age, years	70.7 (7.0)	71.3 (4.8)	71.2 (4.40)	0.894
Male, No. (%)	19 (30.6)	10 (40.0)	5 (50.0)	0.411
Education, years	15.7 (3.9)	15.3 (3.7)	15.3 (3.7)	0.873
APOEε4 carrier, No. (%)	18 (29.0)	12 (48.0)	5 (50.0)	0.156
MMSE score	29.2 (1.2)	28.0 (1.6)[a]	22.5 (4.5)[a,b]	< 0.001
Global Aβ-PET SUVR	1.42 (0.32)	1.96 (0.56)[a]	2.56 (0.4)[a,b]	< 0.001
Temporal meta-ROI tau-PET SUVR	0.77 (0.10)	1.04 (0.41)[a]	2.00 (0.66)[a,b]	< 0.001
Hippocampal volume, cm^3	3.55 (0.39)	3.32 (0.30)[a]	2.58 (0.34)[a,b]	< 0.001
Plasma p-tau217$^+$, pg/mL[c]	0.05 (0.03)	0.11 (0.06)[a]	0.40 (0.32)[a,b]	< 0.001
Follow-up, years	2.3 (0.5)	2.4 (0.6)	2.10 (0.3)[a,b]	0.149

Continuous variables are presented as mean (SD). Analysis of variance (continuous variables) and contingency $\chi 2$ test (categorical variables) tested demographic differences. Tukey's *post hoc* analysis tested significant differences from [a]CU and [b]MCI. [c]Assessed in a subset of 54 individuals (**Supplementary Table 1**). *APOEε4* = Apolipoprotein E ε4; Aβ = amyloid-β; CU = cognitively unimpaired; MMSE = Mini-Mental State Examination; PET = positron emission tomography; p-tau217$^+$ = phosphorylated tau at threonine 217 enhanced by additional phosphorylated sites; ROI = region of interest; SD = standard deviation; SUVR = standardized uptake value ratio.

Table 2. Tau-PET accumulation is accompanied by brain atrophy and clinical decline over time.

	β (95% CI)	*T*-value	*P*-value
Model A: Δ GM density ~ Δ tau-PET SUVR + age + sex + diagnosis + education			
Δ tau-PET SUVR	-0.0009 (-0.0018 to -0.0001)	-2.154	0.034
Age	-0.0003 (-0.0011 to 0.0005)	-0.849	0.398
Male	-0.0005 (-0.0022 to 0.0012)	-0.530	0.598
Diagnosis			
MCI	-0.0004 (-0.0023 to 0.0015)	-0.434	0.665
AD	0.0015 (-0.0020 to 0.0051)	0.862	0.391
Education	-0.00004 (-0.0009 to 0.0008)	-0.095	0.924
Model B: Δ CDR-SB score ~ Δ tau-PET SUVR + age + sex + diagnosis + education			
Δ tau-PET SUVR	0.150 (0.037 to 0.263)	2.648	0.010
Age	0.048 (-0.059 to 0.155)	0.888	0.377
Male	0.111 (-0.112 to 0.334)	0.991	0.325
Diagnosis			
MCI	-0.058 (-0.300 to 0.184)	-0.474	0.637
AD	1.523 (1.035 to 2.012)	6.205	< 0.001
Education	-0.066 (-0.177 to 0.045)	-1.187	0.239

Coefficients and associated statistics from linear regression models testing the association of changes in GM density and CDR-SB score with tau-PET SUVR change adjusting for age, sex, diagnosis, and years of education. Continuous predictors were standardized prior to model entry. Imaging biomarker values were extracted from regions showing *APOE*ε4 and Aβ interaction effects on longitudinal tau-PET accumulation. Analyses involving CDR-SB score were conducted in a subset of 84 individuals. AD = Alzheimer's disease; *APOEε4* = Apolipoprotein E ε4; CDR-SB = clinical dementia rating scale sum of boxes; CU = cognitively unimpaired; GM = grey matter; MCI = mild cognitive impairment; PET = positron emission tomography, p-tau217^{+} = phosphorylated tau at threonine 217 enhanced by additional phosphorylated sites; SUVR = standardized uptake value ratio.

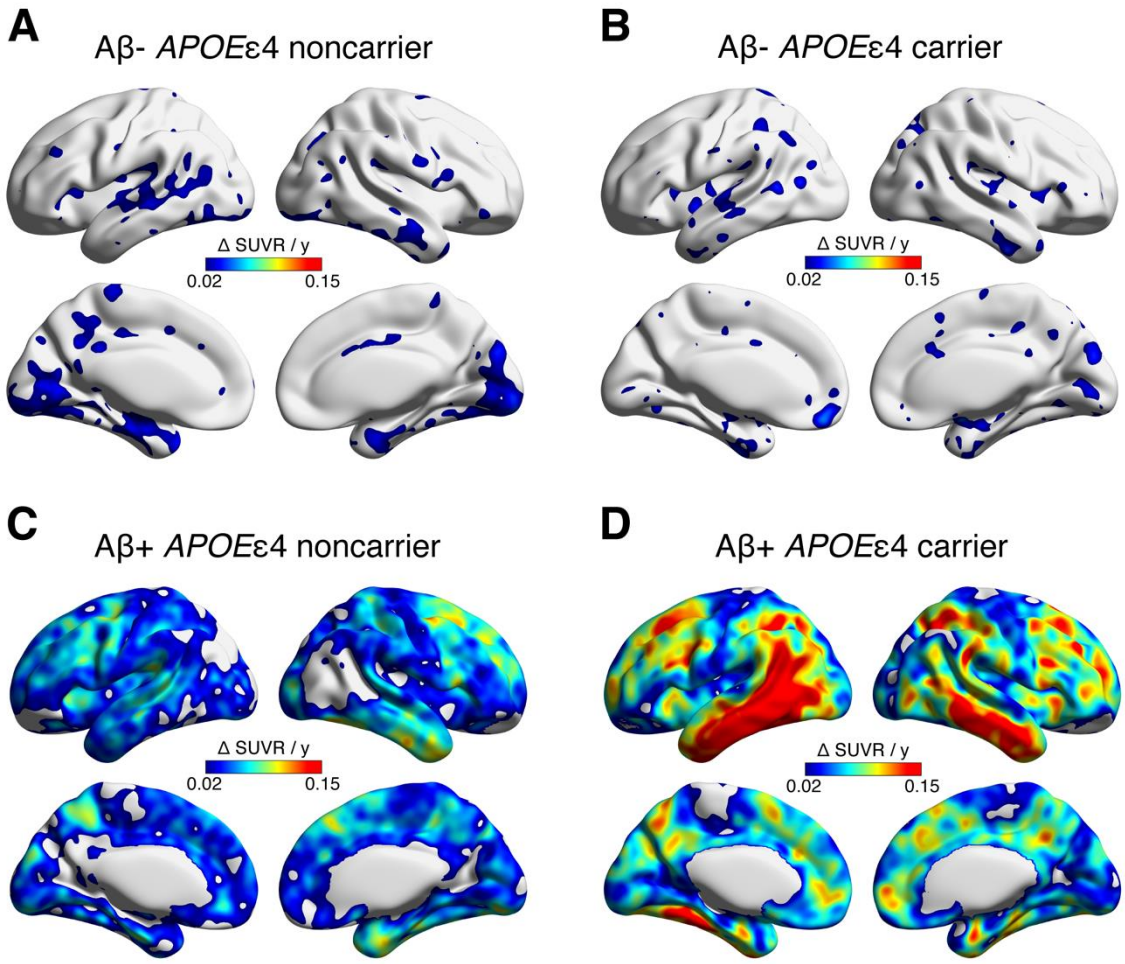

Figure 1. Longitudinal tau-PET accumulation according to *APOE*ε4 and Aβ statuses. Average voxel-wise maps of tau-PET SUVR change per year (ΔSUVR/y) across the following groups: (**A**) Aβ- *APOE*ε4 noncarrier, (**B**) Aβ- *APOE*ε4 carrier, (**C**) Aβ+ *APOE*ε4 noncarrier, and (**D**) Aβ+ *APOE*ε4 carrier.

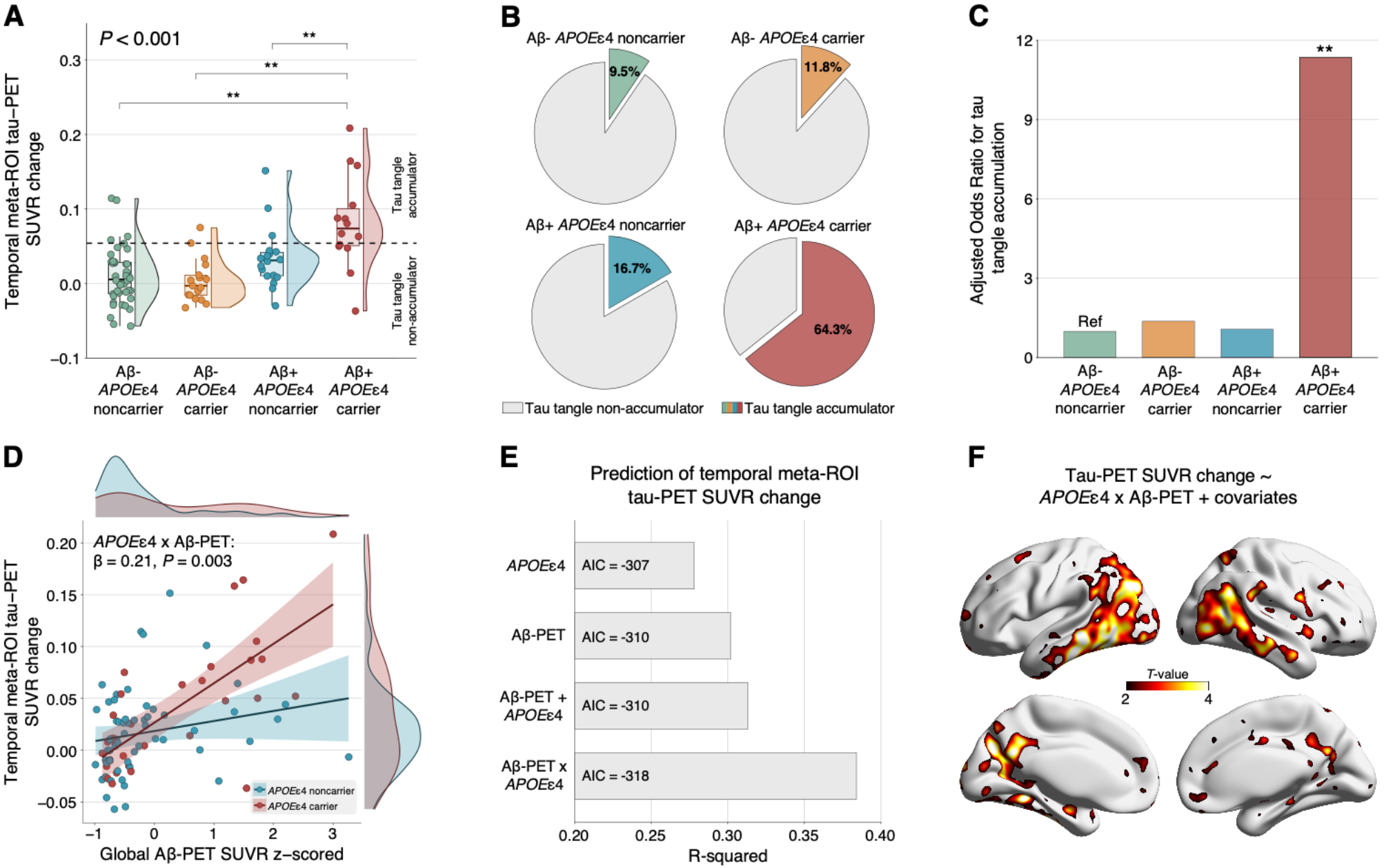
A
P < 0.001
**
**
**
Temporal meta-ROI tau–PET SUVR change
0.3
0.2
0.1
0.0
−0.1
Tau tangle accumulator
Tau tangle non-accumulator
Aβ- APOEε4 noncarrier
Aβ- APOEε4 carrier
Aβ+ APOEε4 noncarrier
Aβ+ APOEε4 carrier
B
Aβ- APOEε4 noncarrier
Aβ- APOEε4 carrier
9.5%
11.8%
Aβ+ APOEε4 noncarrier
Aβ+ APOEε4 carrier
16.7%
64.3%
Tau tangle non-accumulator
Tau tangle accumulator
C
Adjusted Odds Ratio for tau tangle accumulation
12
9
6
3
0
**
Ref
Aβ- APOEε4 noncarrier
Aβ- APOEε4 carrier
Aβ+ APOEε4 noncarrier
Aβ+ APOEε4 carrier
D
APOEε4 x Aβ-PET:
β = 0.21, P = 0.003
Temporal meta-ROI tau–PET SUVR change
0.20
0.15
0.10
0.05
0.00
−0.05
APOEε4 noncarrier
APOEε4 carrier
−1
0
1
2
3
Global Aβ-PET SUVR z–scored
E
Prediction of temporal meta-ROI tau-PET SUVR change
APOEε4
AIC = -307
Aβ-PET
AIC = -310
Aβ-PET + APOEε4
AIC = -310
Aβ-PET x APOEε4
AIC = -318
0.20
0.25
0.30
0.35
0.40
R-squared
F
Tau-PET SUVR change ~
APOEε4 x Aβ-PET + covariates
T-value
2
4

Figure 2. *APOE*ε4 drives Aβ effects on tau tangle accumulation over two years. (**A**) Violin plot of temporal meta-ROI tau-PET SUVR change across groups defined at baseline based on *APOE*ε4 and Aβ statuses. The horizontal line inside each box depicts the median, and box ends represent the 25th and 75th percentiles. The horizontal dashed line represents the threshold for tangle accumulation. Groups were compared using ANCOVA with Tukey's multiple comparison test adjusting for age, sex, and diagnosis (***P* < 0.05). (**B**) Percentage of tau tangle accumulators across groups. (**C**) The figure shows the Odds Ratios across groups from logistic regression analysis on being classified as tau tangle accumulator; the model was adjusted for age, sex, and diagnosis (***P* < 0.05). (**D**) The scatter plot displays the association between global Aβ-PET SUVR and temporal meta-ROI tau-PET SUVR change in *APOE*ε4 noncarriers (blue) and carriers (red). Density plots along the X and Y axes provide the data distribution for global Aβ-PET SUVR and temporal meta-ROI tau-PET SUVR change, respectively. The β-estimate and *P*-value were computed from a regression model assessing the interaction and main effects of *APOE*ε4 status and global Aβ-PET burden on longitudinal tau-PET accumulation accounting for age, sex, and diagnosis. (**E**) R-squared and AIC for different regression models predicting temporal meta-ROI tau-PET SUVR change using either only *APOE*ε4 status, only global Aβ-PET SUVR, both *APOE*ε4 status and global Aβ-PET SUVR, or both *APOE*ε4 status and Aβ-PET SUVR including their interaction term. All models were adjusted for age, sex, and diagnosis. (**F**) *T*-statistical maps from voxel-wise linear regression testing the interaction of *APOE*ε4 status and global Aβ-PET burden on longitudinal tau-PET accumulation adjusting for age, sex, and diagnosis, as well as *APOE*ε4 status and global Aβ-PET burden main effects. Results survived RFT correction for multiple comparisons at $P < 0.05$.

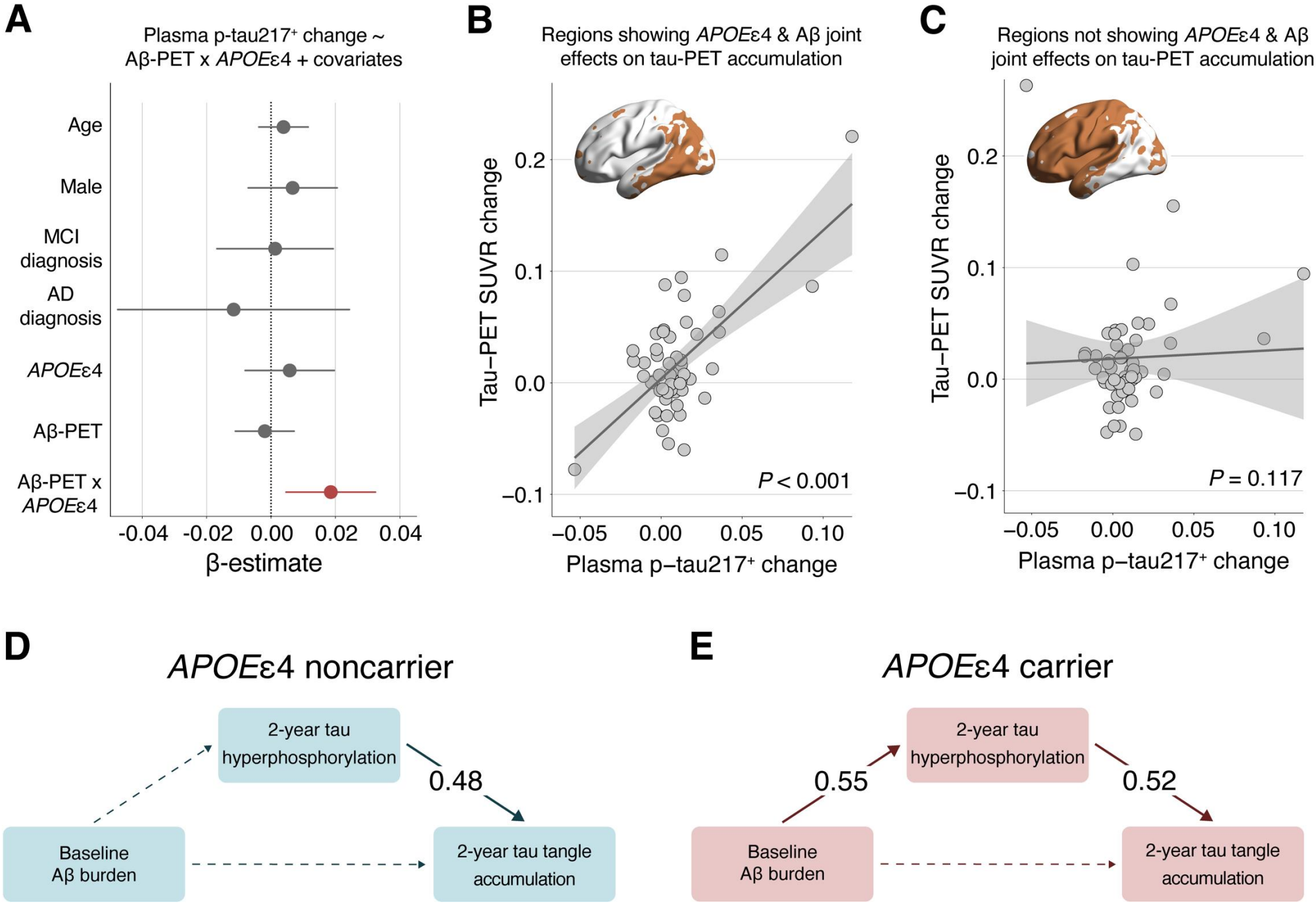
A
Plasma p-tau217+ change ~
Aβ-PET x APOEε4 + covariates
Age
Male
MCI diagnosis
AD diagnosis
APOEε4
Aβ-PET
Aβ-PET x APOEε4
-0.04 -0.02 0.00 0.02 0.04
β-estimate
B
Regions showing APOEε4 & Aβ joint effects on tau-PET accumulation
Tau–PET SUVR change
0.2
0.1
0.0
−0.1
P < 0.001
−0.05 0.00 0.05 0.10
Plasma p–tau217+ change
C
Regions not showing APOEε4 & Aβ joint effects on tau-PET accumulation
Tau–PET SUVR change
0.2
0.1
0.0
−0.1
P = 0.117
−0.05 0.00 0.05 0.10
Plasma p–tau217+ change
D
APOEε4 noncarrier
2-year tau hyperphosphorylation
0.48
Baseline Aβ burden
2-year tau tangle accumulation
E
APOEε4 carrier
2-year tau hyperphosphorylation
0.55
0.52
Baseline Aβ burden
2-year tau tangle accumulation

Figure 3. *APOE*ε4-dependent effects of Aβ on tau tangle accumulation occurs through tau hyperphosphorylation at threonine 217. (**A**) Forest plots showing the β-estimates with 95% CI from regression analysis testing the interaction and main effects of *APOE*ε4 status and global Aβ-PET burden on longitudinal plasma p-tau217^{+} accounting for age, sex, and diagnosis. Red points/lines indicate statistically significant effects on plasma p-tau217^{+} change, whereas grey points/lines represent non-significant associations. The scatter plot shows the association between p-tau217^{+} change and tau-PET SUVR change in (**B**) regions showing *APOE*ε4 and Aβ joint effects on longitudinal tau-PET accumulation and (**C**) regions not showing these joint effects. The β-estimate and *P*-value were computed with a regression model adjusting for age, sex, and diagnosis. Mediation analyses showed that Aβ-PET effects on 2-year tau-PET accumulation occurred through the longitudinal increase of plasma p-tau217+ levels in (**D**) *APOE*ε4 carriers (direct pathway: $P = 0.068$; indirect pathway: $P = 0.018$) but not in (**E**) *APOE*ε4 noncarriers (direct pathway: $P = 0.330$; indirect pathway: $P = 0.560$). Solid lines with standardized β-estimates represent significant associations, whereas dashed lines represent non-significant effects. Aβ burden was measured with global [^{18}F]AZD4694 Aβ-PET SUVR at baseline. Analyses involving longitudinal plasma p-tau217^{+} were conducted in a subset of 54 individuals (**Supplementary Table 1**). Tau tangle accumulation was assessed with [^{18}F]MK-6240 tau-PET SUVR change in the regions showing *APOE*ε4 and Aβ effects on longitudinal tau-PET accumulation. Tau hyperphosphorylation was assessed with plasma p-tau217^{+} change over the follow-up period.

Supplementary Information

Article: "*APOE*ε4 potentiates Aβ effects on longitudinal tangles via tau hyperphosphorylation at threonine 217".

Supplementary Table 1. Demographic comparison between the whole elderly population and the subsample with available longitudinal plasma p-tau217^{+}.

Supplementary Table 2. Demographic characteristics of the CU young population.

Supplementary Table 3. Coefficients and associated statistics from regression analysis testing the association of *APOE*ε4 and Aβ-PET with longitudinal tau-PET accumulation.

Supplementary Table 4. Sensitivity analysis testing the association of *APOE*ε4 and Aβ-PET with longitudinal tau-PET adjusting for baseline tau-PET uptake.

Supplementary Table 5. Sensitivity analysis testing the association of *APOE*ε4 and Aβ-PET with longitudinal plasma p-tau217^{+} adjusting for baseline plasma p-tau217^{+} levels.

Supplementary Table 6. Coefficients and associated statistics from regression analysis testing the longitudinal association of plasma p-tau217^{+} with tau-PET accumulation.

Supplementary Table 7. Sensitivity analysis testing the association of tau-PET accumulation with longitudinal brain atrophy and clinical decline adjusting for baseline GM density and CDR-SB score values, respectively.

Supplementary Figure 1. *APOE*ε4 and Aβ joint effects on tau tangle accumulation were observed in neocortical Braak III-VI regions.

Supplementary Figure 2. Plasma p-tau217^{+} change was not associated with medial temporal tau-PET SUVR change.

Abbreviations: AD = Alzheimer's disease; *APOE*ε4 = apolipoprotein E ε4; Aβ = amyloid-β; CDR-SB = clinical dementia rating scale sum of boxes; CI = confidence interval; CU = cognitively unimpaired; GM = grey matter; MCI = mild cognitive impairment; MMSE = Mini-Mental State Examination; MRI = magnetic resonance imaging; PET = positron emission tomography; p-tau217^{+} = phosphorylated tau at threonine 217 enhanced by additional phosphorylated sites; ROI = region of interest; SUVR = standardized uptake value ratio.

Supplementary Table 1. Demographic comparison between the whole elderly population and the subsample with available longitudinal plasma p-tau217$^+$.

	Whole elderly population	Subsample with longitudinal plasma p-tau217$^+$	*P*-value
No.	91	54	-
Age, years	71.0 (6.4)	71.3 (5.8)	0.793
Male, No. (%)	33 (36.3)	15 (27.8)	0.294
Education, years	15.6 (3.9)	15.7 (3.7)	0.855
APOEε4 carrier, No. (%)	31 (34.1)	18 (33.3)	0.938
Diagnosis, No. (%)			
CU	62 (68.1)	35 (64.8)	
MCI	23 (25.3)	17 (31.5)	0.594
AD	6 (6.6)	2 (3.7)	
MMSE score	28.4 (2.4)	28.5 (2.6)	0.881
Global Aβ-PET SUVR	1.63 (0.54)	1.67 (0.54)	0.699
Temporal meta-ROI tau-PET SUVR	0.90 (0.38)	0.91 (0.36)	0.811
Hippocampal volume, cm^3	3.44 (0.43)	3.46 (0.39)	0.821
Follow-up, years	2.4 (0.5)	2.3 (0.4)	0.661

Continuous variables are presented as mean (SD). Student's t test (continuous variables) and contingency $\chi 2$ test (categorical variables) tested demographic differences. Of note, the whole elderly population does not include the outliers (n = 6) and the CU young population (n = 10) because these individuals were not included in our statistical analyses.

Supplementary Table 2. Demographic characteristics of the CU young population.

	CU young
No.	10
Age, years	22.1 (1.4)
Male, No. (%)	4 (40.0)
Education, years	15.8 (1.5)
APOEε4 carrier, No. (%)	1 (10.0)
MMSE score	29.8 (0.6)
Global Aβ-PET SUVR	1.21 (0.07)
Temporal meta-ROI tau-PET SUVR	0.68 (0.09)
Hippocampal volume, cm^3	4.22 (0.55)
Follow-up, years	2.5 (0.6)

Continuous variables are presented as mean (SD).

Supplementary Table 3. Coefficients and associated statistics from regression analysis testing the association of *APOE*ε4 and Aβ-PET with longitudinal tau-PET accumulation.

	β (95% CI)	*T*-value	*P*-value
Δ tau-PET SUVR ~ *APOE*ε4 status*Aβ-PET SUVR + age + sex + diagnosis			
*APOE*ε4 carriership	0.009 (-0.010 to 0.027)	0.946	0.347
Aβ-PET SUVR	0.001 (-0.012 to 0.015)	0.202	0.841
Age	-0.001 (-0.009 to 0.008)	-0.199	0.842
Male	0.010 (-0.008 to 0.028)	1.109	0.271
Clinical diagnosis			
MCI	0.014 (-0.008 to 0.037)	1.273	0.207
AD	0.047 (0.003 to 0.091)	2.109	0.038
*APOE*ε4 carriership x Aβ-PET SUVR	0.027 (0.010 to 0.045)	3.091	0.003

Continuous predictors were standardized prior to model entry. Aβ-PET was assessed in the global neocortical composite, and tau-PET was assessed in the temporal meta-ROI. All predictors were assessed at the baseline visit.

Supplementary Table 4. Sensitivity analysis testing the association of *APOE*ε4 and Aβ-PET with longitudinal tau-PET adjusting for baseline tau-PET uptake.

	β (95% CI)	*T*-value	*P*-value
Δ tau-PET SUVR ~ *APOE*ε4 status*Aβ-PET SUVR + age + sex + diagnosis + baseline tau-PET SUVR			
*APOE*ε4 carriership	0.009 (-0.009 to 0.028)	1.026	0.308
Aβ-PET SUVR	0.004 (-0.011 to 0.019)	0.550	0.584
Age	-0.001 (-0.010 to 0.008)	-0.254	0.800
Male	0.009 (-0.009 to 0.027)	1.023	0.309
Clinical diagnosis			
MCI	0.016 (-0.007 to 0.038)	1.396	0.167
AD	0.060 (0.009 to 0.112)	2.339	0.022
Baseline tau-PET SUVR	-0.007 (-0.020 to 0.006)	-1.025	0.308
*APOE*ε4 carriership x Aβ-PET SUVR	0.027 (0.009 to 0.044)	3.025	0.003

Continuous predictors were standardized prior to model entry. Aβ-PET was assessed in the global neocortical composite, and tau-PET was assessed in the temporal meta-ROI. All predictors were assessed at the baseline visit.

Supplementary Table 5. Sensitivity analysis testing the association of *APOE*ε4 and Aβ-PET with longitudinal plasma p-tau217$^+$ adjusting for baseline plasma p-tau217$^+$ levels.

	β (95% CI)	*T*-value	*P*-value
Δ plasma p-tau217$^+$ ~ *APOE*ε4 status*Aβ-PET SUVR + age + sex + diagnosis + baseline plasma p-tau217$^+$			
*APOE*ε4 carriership	0.008 (-0.005 to 0.021)	1.290	0.204
Aβ-PET SUVR	0.001 (-0.008 to 0.011)	0.316	0.753
Age	0.004 (-0.003 to 0.010)	1.171	0.248
Male	0.006 (-0.008 to 0.019)	0.831	0.410
Clinical diagnosis			
MCI	0.002 (-0.014 to 0.017)	0.216	0.830
AD	0.016 (-0.032 to 0.065)	0.670	0.506
Baseline plasma p-tau217$^+$	-0.009 (-0.020 to 0.002)	-1.587	0.119
*APOE*ε4 carriership x Aβ-PET SUVR	0.019 (0.006 to 0.032)	2.977	0.005

Continuous predictors were standardized prior to model entry. Aβ-PET was assessed in the global neocortical composite. All predictors were assessed at the baseline visit.

Supplementary Table 6. Coefficients and associated statistics from regression analysis testing the longitudinal association of plasma p-tau217$^+$ with tau-PET accumulation.

	β (95% CI)	*T*-value	*P*-value
Δ tau-PET SUVR ~ Δ plasma p-tau217$^+$ + age + sex + diagnosis			
Δ plasma p-tau217$^+$	0.033 (0.022 to 0.044)	6.008	< 0.001
Age	-0.004 (-0.015 to 0.008)	-0.624	0.536
Male	-0.014 (-0.037 to 0.009)	-1.205	0.234
Clinical diagnosis			
MCI	0.014 (-0.009 to 0.037)	1.249	0.218
AD	0.034 (-0.019 to 0.088)	1.302	0.199

Continuous predictors were standardized prior to model entry. Aβ-PET was assessed in the global neocortical composite, and tau-PET was assessed in the regions showing *APOE*ε4 and Aβ joint effects on longitudinal tau-PET accumulation.

Supplementary Table 7. Sensitivity analysis testing the association of tau-PET accumulation with longitudinal brain atrophy and clinical decline adjusting for baseline GM density and CDR-SB score values, respectively.

	β (95% CI)	*T*-value	*P*-value
Model A: Δ GM density ~ Δ tau-PET SUVR + age + sex + diagnosis + education + baseline GM density			
Δ tau-PET SUVR	-0.0010 (-0.0018 to -0.0002)	-2.386	0.019
Age	-0.0008 (-0.0016 to 0.00002)	-1.930	0.057
Male	0.0009 (-0.0009 to 0.0028)	0.978	0.331
Diagnosis			
MCI	-0.0006 (-0.0024 to 0.0012)	-0.672	0.503
AD	-0.0004 (-0.0040 to 0.0032)	-0.220	0.827
Education	-0.000004 (-0.0008 to 0.0008)	-0.010	0.992
Baseline GM density	-0.0014 (-0.0024 to -0.0005)	-3.014	0.003
Model B: Δ CDR-SB score ~ Δ tau-PET SUVR + age + sex + diagnosis + education + baseline CDR-SB score			
Δ tau-PET SUVR	0.171 (0.079 to 0.263)	3.690	< 0.001
Age	0.034 (-0.054 to 0.122)	0.773	0.442
Male	-0.004 (-0.190 to 0.181)	-0.046	0.963
Diagnosis			
MCI	0.313 (0.083 to 0.543)	2.710	0.008
AD	2.865 (2.281 to 3.449)	9.776	< 0.001
Education	-0.061 (-0.152 to 0.029)	-1.347	0.182
Baseline CDR-SB score	-0.442 (-0.582 to -0.301)	-6.277	< 0.001

Coefficients and associated statistics from regression models testing the association of changes in GM density and CDR-SB score with tau-PET SUVR change adjusting for age, sex, diagnosis, years of education, and baseline GM density (Model A) or CDR-SB score (Model B). Continuous predictors were standardized. Imaging biomarker values were extracted from regions showing *APOE*ε4 and Aβ interaction effects on longitudinal tau-PET accumulation. CDR-SB analysis was conducted in a subset of 84 individuals with longitudinal CDR-SB data.

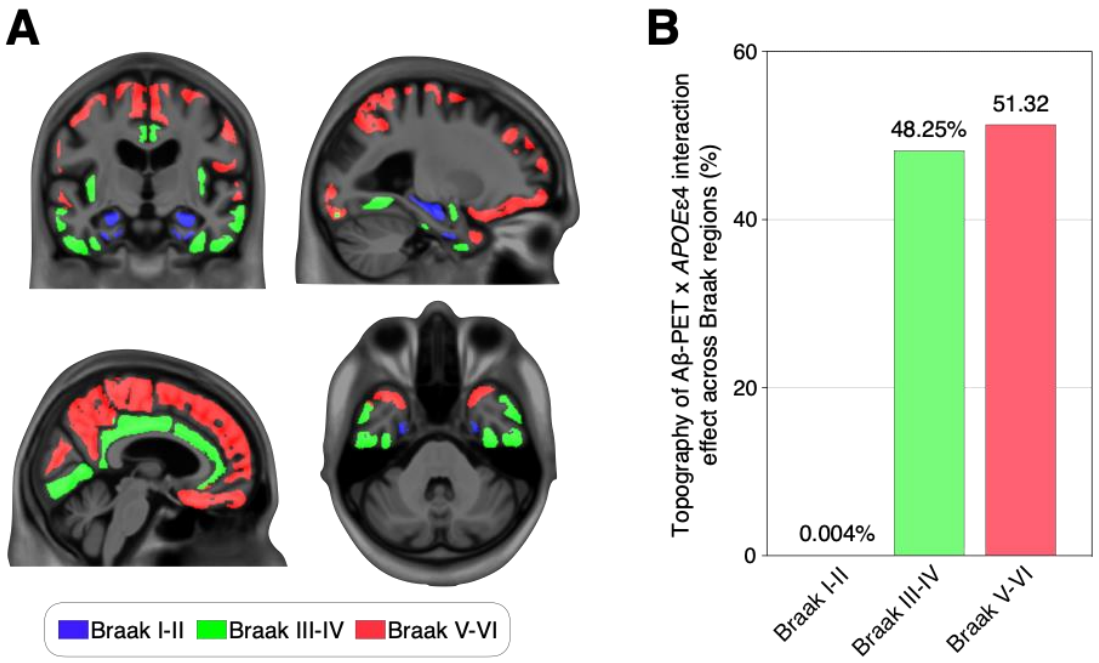

Supplementary Figure 1. *APOE*ε4 and Aβ joint effects on tau tangle accumulation were observed in neocortical Braak III-VI regions. (**A**) Representation of Braak-like stages ROIs overlaid on a structural MRI template. (**B**) The bar plot indicates the topography (% area) of *APOE*ε4 carriership and global Aβ-PET load interaction effects on longitudinal tau-PET SUVR increase across Braak-like stage regions.

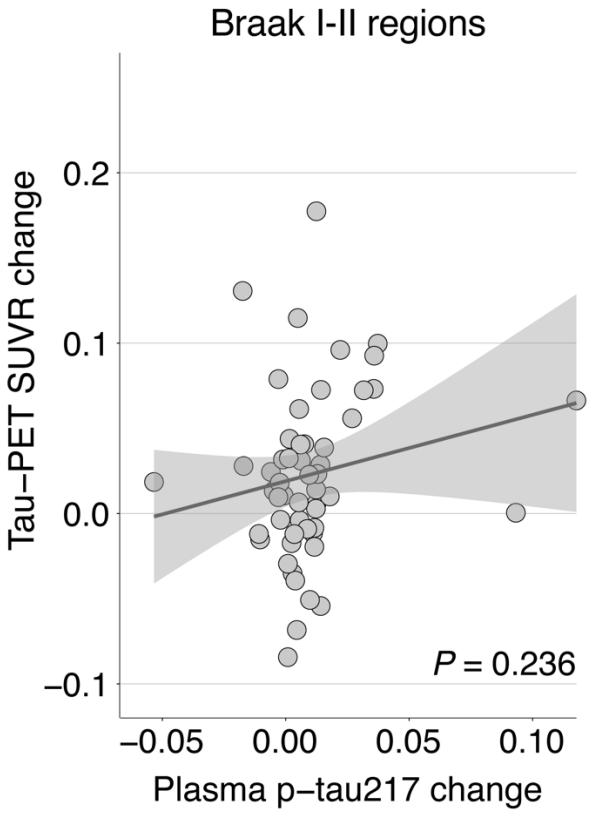

Supplementary Figure 2. Plasma p-tau217^{+} change was not associated with medial temporal tau-PET SUVR change. The scatter plot shows the association between p-tau217^{+} change and tau-PET SUVR change in Braak I-II regions, which comprise the transentorhinal, entorhinal and hippocampus. The β-estimate and *P*-value were computed with a regression model adjusting for age, sex, and diagnosis. Importantly, we selected Braak I-II regions as a representative brain area because it almost did not show fast tau accumulation related to *APOE*ε4 and Aβ joint effects (0.004% area affected), as depicted in **Supplementary Figure 1B**. This further supports that the longitudinal association between tau-PET accumulation and plasma p-tau217^{+} increase over the follow-up period was mainly restricted to brain areas showing *APOE*ε4 and Aβ joint effects on tau-PET accumulation.